



Universiteit
Leiden
The Netherlands

Unraveling the synergistic role of ABA and ethylene in root lignin synthesis: a key molecular mechanism for tobacco response to PS-NPs using multi-omics approaches

Jia, T.; Sun, X.; Li, W.; Chen, J.; Peijnenburg, W.J.G.M.; Liu, P.; Yang, L.

Citation

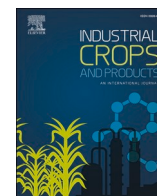
Jia, T., Sun, X., Li, W., Chen, J., Peijnenburg, W. J. G. M., Liu, P., & Yang, L. (2025). Unraveling the synergistic role of ABA and ethylene in root lignin synthesis: a key molecular mechanism for tobacco response to PS-NPs using multi-omics approaches. *Industrial Crops And Products*, 233. doi:10.1016/j.indcrop.2025.121356

Version: Publisher's Version

License: [Creative Commons CC BY 4.0 license](https://creativecommons.org/licenses/by/4.0/)

Downloaded from: <https://hdl.handle.net/1887/4252240>

Note: To cite this publication please use the final published version (if applicable).



Unraveling the synergistic role of ABA and ethylene in root lignin synthesis: A key molecular mechanism for tobacco response to PS-NPs using multi-omics approaches

Tao Jia^a, Xiaodong Sun^a, Wenwen Li^a, Jingrui Chen^a, Willie J.G.M. Peijnenburg^{b,c}, Peng Liu^{a,*}, Long Yang^{a,*}

^a College of Plant Protection, Shandong Agricultural University, Taian 271000, China

^b Institute of Environmental Sciences (CML), Leiden University, P.O. Box 9518, Leiden 2300 RA, the Netherlands

^c National Institute of Public Health and the Environment (RIVM), P.O. Box 1, Bilthoven, the Netherlands

ARTICLE INFO

Keywords:

Lignin
Multi-omics
Plant hormone
PS-NPs

ABSTRACT

The widespread of plastics poses health risks through the food chain. While plenty of studies show plants absorb it through roots, but research on root responses to it is limited. This study explored the molecular mechanisms of tobacco seedling roots response to different polystyrene nanoparticles (PS-NPs) concentrations using multi-omics approaches. The results from confocal laser scanning microscopy indicated PS-NPs accumulate in root was proportional to concentration. PS-NPs reduced fresh weight by 19.1, 37.0, and 49.7 % in accompanied by increasing ROS. It is noteworthy that the lignin content was also significantly influenced, exhibiting an increase at low concentrations of PS-NPs and a decrease at high concentrations of PS-NPs. Compared to the control, the lignin content is 1.02, 0.87, and 0.83 times that of the control, respectively. To clarify the molecular mechanisms influencing the lignin content, a joint analysis of transcription-metabolism was conducted. It was found that ABA-related metabolites and genes first increased then decreased. In contrast, ethylene, which promote lignin degradation, showed an upward trend. It is likely that the dynamic balance between ABA and ethylene may influence lignin synthesis under PS-NPs treatment. This contribution not only clarified the impact of PS-NPs on plant root growth but also elucidated the potential mechanisms of phytotoxicity.

1. Introduction

In 1907, The appearance of synthetic plastic resins altered daily life, embedding plastics deeply into human activities due to their versatility. However, in the course of the 20th century, plastics were identified as major pollutants affecting diverse environments. The term "microplastic" was introduced by Thompson et al. in 2004 and quickly gained prominence. MPs can be divided into "primary MPs" and "secondary NPs" (Ali et al., 2021). Primary MPs are manufactured directly from industrial production, such as plastic particles used in paints, adhesives, electronics, and cosmetics. Secondary NPs are smaller plastic particles formed by the decomposition of larger plastic waste through environmental transformations actions like photolysis and mechanical decomposition (Arif et al., 2024).

Due to their tiny size, MPs/NPs can be widely distributed in the environment and accumulate in soil, air, water (Da Costa et al., 2016).

MPs/NPs induce toxicity to living organisms, potentially impacting their growth and development, even causing their death (Zhao et al., 2023a). MPs/NPs have for example been found to cause lethal and sublethal effects on zebrafish embryos (Lee et al., 2023), and were shown to enter the human body through food ingestion, respiratory inhalation, or skin contact (Li et al., 2024). MPs/NPs can trigger oxidative stress, inflammation, and tissue damage, increasing the risk of neurodegenerative diseases, reproductive problems, heart disease, cancer, and autoimmune diseases (Ramos-González et al., 2024). In addition, it has been found that MPs/NPs can be absorbed and accumulated by terrestrial plants (Gan et al., 2023). Although the absorption of MPs/NPs by leaves is one of the pathways for their entry into plants, the primary means of absorption is through the roots, where they accumulate predominantly (Hua et al., 2023). The concentration of MPs/NPs in the roots reached significant levels, and then subsequently transported through the xylem to the aboveground parts. The accumulation of MPs/NPs could inhibit

* Correspondence to: Associate Professor of College of Plant Protection, Shandong Agricultural University, No. 61 Daizong street, Taian, Shandong 271018, China
E-mail addresses: liupeng2003@sdau.edu.cn (P. Liu), lyang@sdau.edu.cn (L. Yang).

seed germination and plant growth through altering antioxidant enzyme activity, gene expression, and metabolite composition in different species. Research to date has established that the primary transport pathway for MPs/NPs from the root surface to the xylem is through the apoplast. The apoplast is primarily composed of cavities formed by cell walls and intercellular spaces, which present minimal resistance and facilitate rapid, uniform transport of inorganic ions and organic substances (Zhang et al., 2023). The transport rate within the apoplast is indeed influenced by the structure of the cell wall (Schreiber et al., 1999). Lignin is a crucial component of plant cell walls, primarily serving to enhance their mechanical strength and acting as a physical barrier that participates in plant defense responses (Riseh et al., 2024). Changes in lignin content are especially an important mechanism for plants to resist adversity when plants encounter harmful substance stress such as heavy metal and salt (Na^+) stress.

Throughout their long evolutionary history, plants have cultivated intricate defense mechanisms to counteract harsh environmental conditions. Plant hormones, present in trace amounts, are organic substances that significantly regulate plant growth and development. An increasing body of research indicates that abscisic acid (ABA) and ethylene are integral to how plants react to various stressors, such as low temperatures, elevated salinity levels, and assaults by pathogens (Dar et al., 2017; Zahra et al., 2023). The primary function of ABA is to regulate stomatal opening and closing by modulating ion channels and pumps in guard cells, thereby influencing the internal water status and photosynthesis. The primary role of ethylene is to inhibit the vegetative growth of plants and promote reproductive growth through signal transduction when plants encounter stress conditions (Ogawara et al., 2003). Extensive research has demonstrated a close relationship between these two hormones and the synthesis and decomposition of lignin under stress conditions. Among them, ABA had been widely proven to significantly enhance lignin synthesis (Liu et al., 2021). As for ethylene, its effect on lignin content is twofold, meaning that under different conditions, it may either promote synthesis or decomposition of lignin (Barberon et al., 2016; Torres et al., 2020). However, to date, there is still a lack of research on the relationship and regulatory mechanisms between plant root hormones and lignin metabolism following exposure to MPs/NPs. Based on our preliminary studies, we hypothesized that under MPs/NPs stress, the dynamic balance of plant hormones regulated lignin biosynthesis in tobacco roots, thereby enhancing plant resistance to MPs/NPs.

Tobacco is one of the most important economic crops around the world. Despite the health risks associated with smoking, the economic benefits have prevented the implementation of a smoking ban. It is well known that tobacco smoke contains plenty of harmful components such as nicotine, tobacco tar, and carbon monoxide. These toxicants not only directly impact smokers' health but can also persist as third-hand smoke in the environment, posing significant risks to especially infants and children. Recent research indicated that MPs/NPs were existed in sample of bronchoalveolar lavage fluid (BALF) of smokers. Smokers exhibited elevated concentrations of total microplastics, polyurethane, and silicone when compared to non-smokers (Lu et al., 2023). Another case study examined the presence of MPs/NPs in the sputum of 22 patients, comprising both smokers and non-smokers. The results indicated that, compared to non-smokers, the concentration of MPs/NPs in the sputum significantly increased among long-term smokers (Huang et al., 2022). Consequently, analyzing the mechanisms by which tobacco absorb MPs/NPs, along with an in-depth exploration of potential resistance mechanisms, is of great significance for reducing the accumulation of MPs/NPs and mitigating their harmful effects on human health. This study utilizes the tobacco variety NC55, which is widely cultivated in China, as the research material. Through a comprehensive analysis of transcription, metabolism, and physiology, the dynamic trends in tobacco root absorption of PS-NPs are revealed and we uncover the molecular mechanisms within tobacco that enhance its resistance to PS-NPs. This comprehensive methodology could yield novel insights

into the impact of MPs/NPs on agricultural crops and potentially identify more robust targets for genetic modification. Such advancements could be pivotal in enhancing crops' resilience against the detrimental effects of MPs/NPs.

2. Materials and methods

2.1. Phenotype of PS-NPs

PS-NPs fluorescent nanospheres were provided by Jiangsu Ishikawa Technology Co., Ltd. The particle size distribution, morphology, and appearance of the target particles were analyzed by Transmission Electron Microscopy (Talos L120C TEM).

2.2. Experimental materials and growth conditions

NC55 tobacco (*Nicotiana tabacum* L.) seeds were germinated in seedling trays. After seed germination, healthy and uniform seedlings were transplanted into 1/2 Hoagland solution with four treatments: Control (CK), 10, 50, and 100 $\text{mg}\cdot\text{L}^{-1}$ of PS-NPs. The seedlings were cultured in an incubator under light intensity of 4000 lx, at a temperature range of 28–30°C. The photoperiod was 16 h/8 h, with humidity maintained at 60 %.

2.3. Root growth

After being sampled, the entire seedlings were thoroughly rinsed with distilled water to measure fresh and dry weights of shoots and roots respectively. The total root length, root diameter, and number of root bifurcations were analyzed using root scanner (Shanghai Zhongjing Technology Co., Ltd., China).

2.4. Enzyme activity assay, DAB, and NBT staining

POD, SOD, CAT, and APX, along with MDA content, were determined using a detection kit from Solarbio Science & Technology Co., Ltd., following the manufacturer's instructions. The staining procedures with DAB and NBT were performed according to established methods, with specific steps detailed in the [supplementary materials](#) (Text S1).

2.5. Confocal Laser Scanning Microscopy (CLSM)

Root specimens were gathered for examination via Confocal Laser Scanning Microscopy (CLSM) to ascertain the possible deposition of PS-NPs within the root systems. Initially, the roots were meticulously rinsed with deionized water to eliminate any PS-NPs adhering to the exterior. Subsequently, the root tips were mounted on a glass slide with deionized water and secured under a cover slip. The specimens were then subjected to thorough analysis using a confocal laser scanning microscope model Leica TCS SP8, provided by Leica Microsystems. The imaging was facilitated by the LAS X software version 3.5.6.21594, also from Leica Microsystems. During the entire process, a wavelength of 535 nm was used for excitation, while a wavelength of 610 nm was utilized for emission. To maintain uniformity across the analysis, each image was recorded using identical parameters.

2.6. Quantification of lignin content in tobacco

A 0.5 g sample was combined with 95 % ethanol, then ground to form a uniform mixture. Which was subsequently centrifugation at 2600 g for a duration of 5 min to isolate the solid residue, known as the pellet. The pellet was subsequently washed with 95 % ethanol twice and with a mixture of ethanol and n-hexane (in a 1:2 ratio) twice to ensure purification, followed by air-drying. Once dry, the pellet was combined with 25 % solution of bromoacetyl glacial acetic acid and allowed to dissolve in 70°C water bath for 30 min. Subsequently, the solution was

treated with 0.9 mL of 2 M sodium hydroxide, 5 mL of pure acetic acid, and 0.1 mL of 7.5 M hydroxylamine hydrochloride, and then diluted to total volume with an additional 15 mL of pure acetic acid. The concentration of lignin in the original sample was ascertained by measuring the absorbance of the supernatant at a wavelength of 280 nm.

2.7. RNA extraction and transcriptomic analysis

Total root tissue RNA was isolated using the RNeasy Pure Plant Kit, with purity and concentration assessed via absorbance and electrophoresis. High-quality RNA samples were sequenced and analyzed to determine gene expression patterns in tobacco root tissues. For detailed methods, see the [supplementary materials](#) (Text S2).

2.8. Metabolomics analysis

A standardized protocol (Wu et al., 2024) was used for the metabolic profiling. The specific steps and parameter settings of the experiment have been documented in detail in an attached file (Text S3). Samples were accurately weighed, using specific extraction and homogenization techniques, as well as a series of centrifugation and cooling steps to separate and purify the target components. Chromatographic conditions and mass spectrometry parameters followed the recommended settings in the literature to ensure accuracy and reproducibility of the analysis. To further ensure the reliability of the experimental results, we performed quality control (QC) analysis on all samples and mixed equal amounts of samples to form QC samples. In addition, specialized software tools are used for the processing of raw data and the identification of metabolites.

2.9. Weighted gene co-expression network analysis (WGCNA)

The *hclust* function in R language was used for systematic cluster analysis, and the WGCNA package was used to construct weighted gene co-expression network in tobacco roots, and the correlation analysis of genes and modules, genes and the biological enzyme activities was carried out. According to the characteristic heat map of the clustering module obtained from WGCNA analysis, the specific method was referred to by Zhang et al. (2023). Further details are provided in the [supplementary information](#) (Text S4).

2.10. Quantitative real-time PCR (qRT-PCR) validation

For this particular experiment, we employed a unique collection of samples for qRT-PCR analysis, focusing on RNA isolated from the root tips of young seedlings. The procedural steps followed the experimental design detailed in our preceding research, which included the extraction of total RNA, the generation of first-strand complementary DNA (cDNA), and the execution of qRT-PCR analysis. The precise sequences of the PCR primers utilized are detailed in Table S1 of the [Supplementary Materials](#) (Text S5).

2.11. Data analysis

All experimental procedures were replicated four times to guarantee both reliability and consistency of the results. The data were presented as the mean value plus or minus the standard deviation (mean \pm SD). Statistical analysis was performed using one-way analysis of variance (ANOVA) with a significance threshold set at 0.05 ($p < 0.05$), utilizing SPSS software version 17.0 by IBM, USA, followed by Tukey's honestly significant difference (HSD) test for post hoc comparisons. The visualization of the results was accomplished with Origin 2021 software. The correlation between experimental results was assessed using Pearson correlation analysis. The data were analyzed using the SAS 9.4 (SAS Institute Inc., Cary, NC, USA). The partial least squares path model (PLS-PM) was used to confirm the correlation between antioxidants, NPs,

lignin, and plant stem biomass and root biomass.

3. Results

3.1. Phenotype of PS-NPs

The PS-NPs were spherical particles with a solid matter content of the initial suspensions of 2.5 % and a density of 1.05 g/cm³. These PS-NPs included PS nanospheres that were fluorescently labeled with a red dye. When excited at 535 nm wavelength, these nanospheres emitted bright fluorescence at 610 nm. The concentration of these PS-NPs nanospheres was 25 mg·mL⁻¹. The specific particle size distribution was depicted in Fig. 1.

3.2. Effect of PS-NPs on tobacco seedlings growth

As the concentration of PS-NPs escalated, there was notable decline in plant growth, as depicted in Fig. 2A. The reduction in root fresh weight was 24.29 % at dosage of 10 mg·L⁻¹, and this decrease became more pronounced at 43.88 % and 66.27 % for concentrations of 50 and 100 mg·L⁻¹, respectively (Fig. 2B). In a similar vein, the fresh weight of the shoots also diminished with increasing PS-NPs concentration, showing decreases of 19.11 %, 37.00 %, and 49.66 % at 10, 50, and 100 mg·L⁻¹ (Fig. 2C). The dry weight of the roots was reduced by 17.82 % at PS-NPs concentration of 10 mg·L⁻¹, with more significant reductions of 45.27 % and 70.02 % at 50 and 100 mg·L⁻¹ concentrations (Fig. 2D). Correspondingly, the dry weight of the shoots also experienced decline, with reductions of 28.90 %, 47.80 %, and 61.14 % under the varying treatment conditions (Fig. 2E). As the treatment concentration rose, leaf area (Fig. S1A), leaf length (Fig. S1B), and root length (Fig. S1C) of the PS-NPs groups decreased. Average root diameter also decreased by 12.23 %, 20.83 %, and 26.72 % for these groups. Notably, the 100 mg·L⁻¹ PS-NPs treatment showed the greatest decrease in plant growth index (Fig. S1D), suggesting more pronounced inhibitory effect of higher concentrations.

3.3. Changes in antioxidant enzyme content

DAB and NBT staining revealed that the roots exhibited an expansion and intensification of brown and blue discolorations with escalating concentrations of PS-NPs, in contrast to the control group (Fig. 3A and B). MDA levels showed pronounced elevation, with increments of 151.0 %, 294.8 %, and 441.5 % corresponding to the 10, 50, and 100 mg·L⁻¹ treatments, respectively (Fig. 3C). Antioxidant enzyme activities within the plants were significantly affected by the increasing PS-NPs concentrations. CAT, POD, and APX activities all demonstrated upward trend with rising PS-NPs levels. Specifically, CAT activity escalated by 34.08 %, 57.49 %, and 88.79 % for the 10, 50, and 100 mg·L⁻¹ treatments (Fig. 3D). APX activity followed a similar pattern, increasing by 19.35 %, 41.18 %, and 74.09 % under the same treatment conditions (Fig. 3E). POD activity also rose, with increases of 37.27 %, 52.86 %, and 110.16 % at the 10, 50, and 100 mg·L⁻¹ treatments (Fig. 3F). In contrast, SOD activity was notably reduced with the increasing presence of PS-NPs (Fig. 3G). RDA revealed a strong association between data such as enzyme activity and physiology in plant roots and processing variables. Especially the sample points for APX, CAT, and POD in the PS50 and PS100 groups cluster tightly on the positive RDA1 axis, indicating a positive correlation among these variables specifically within these groups. This trend suggests under high PS-NPs treatment conditions, these three antioxidant enzymes (APX, CAT, and POD) may occupy relatively prominent position (Fig. 4).

3.4. Distribution and accumulation of PS-NPs in tobacco roots

Tobacco was able to absorb PS-NPs through its root system. However, there were differences in the PS-NPs accumulation at different

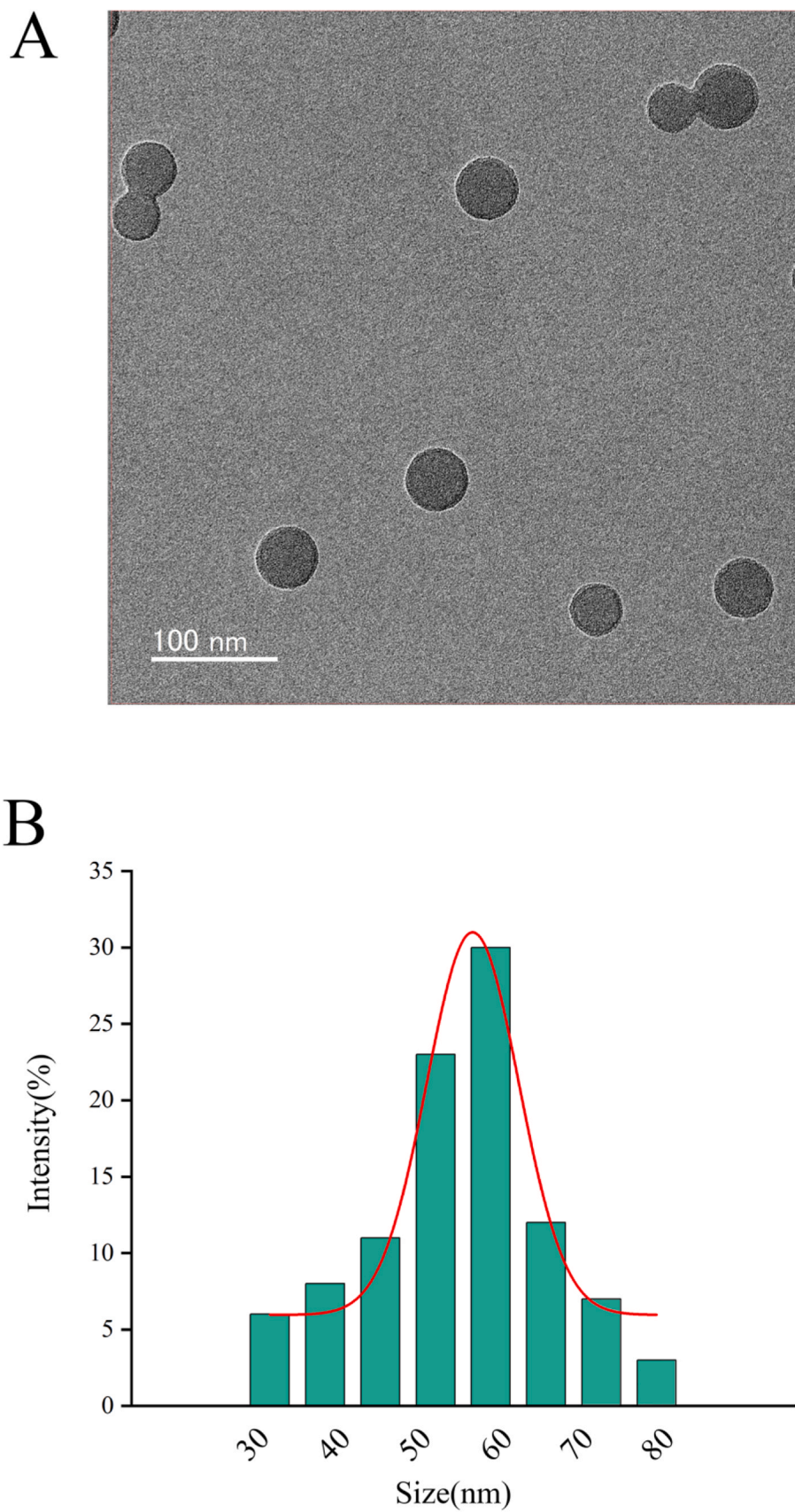


Fig. 1. Characterization of PS-NPs (A) SEM image; (B) Size distribution of the PS-NPs particles.

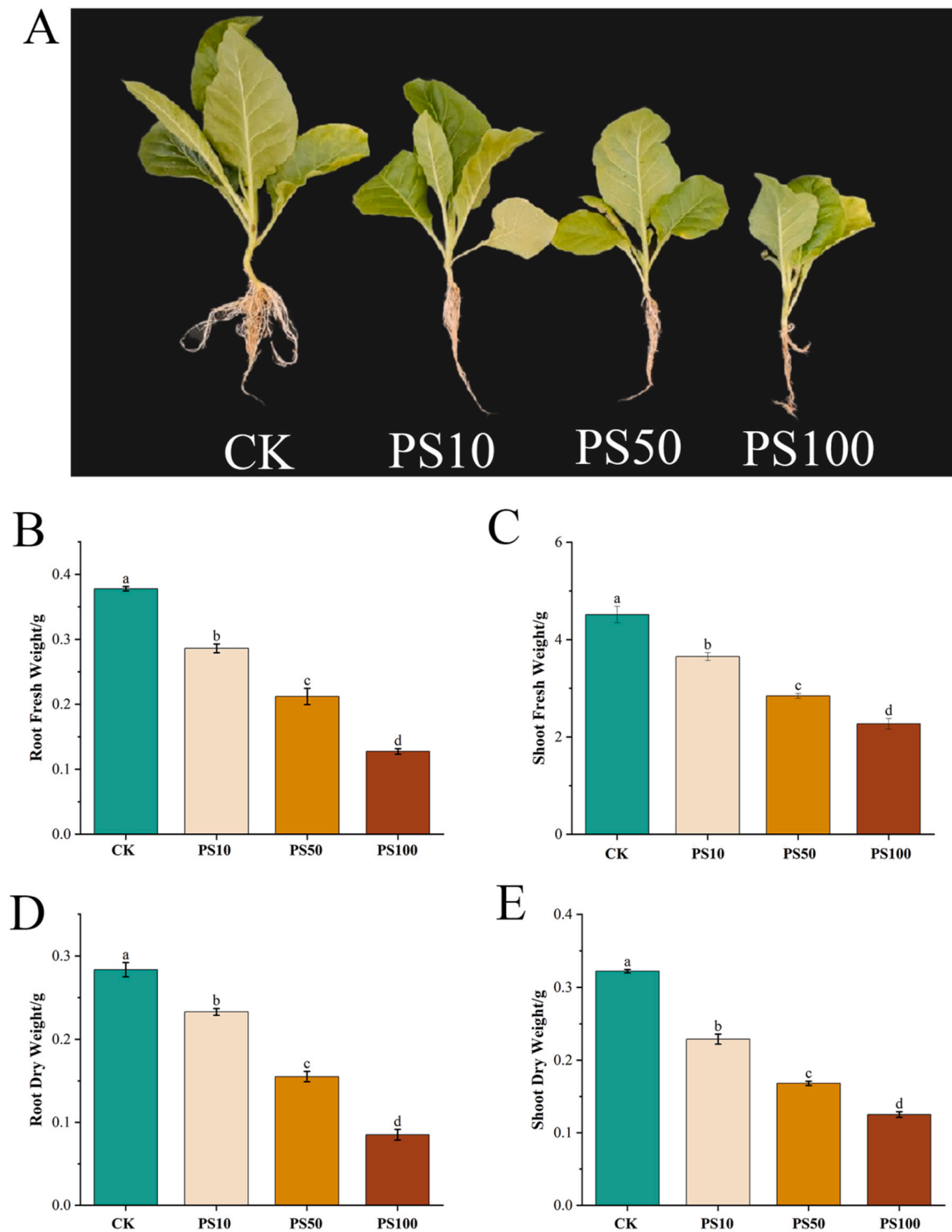


Fig. 2. The effect of different PS-NPs concentrations on plant growth (A) Phenotype diagram; (B) Root fresh weight; (C) Shoot fresh weight; (D) Root dry weight; (E) Shoot dry weight.

concentrations. 100 mg·L⁻¹ and 50 mg·L⁻¹ tobacco root scans were darker. The higher the exposure concentration of PS-NPs, the stronger the red fluorescence intensity (Fig. 5A-B).

3.5. Root transcriptomic analysis of plants exposed to PS-NPs

The PCA results indicated strong clustering within the same treatments and clear separation between different treatments. This demonstrated the high accuracy and reliability of the transcription data (Fig. 6

A). A total of 7314 common differentially expressed genes (DEGs) were covered in the three comparison groups, with 4238, 673, and 1622 DEGs specific to PS10 vs CK, PS50 vs CK, and PS100 vs CK (Fig. 6B). In the PS10 vs CK comparison, 5685 genes showed differential expression, with 1870 up and 3815 down (Fig. 6C). For PS50 vs CK, 2046 genes were differentially expressed, including 1253 up and 793 down (Fig. 6D). In the PS100 vs CK group, 3671 genes were differentially expressed, with 2167 up and 1504 down (Fig. 6E).

KEGG compared three different PS-NPs treatment groups (PS10,

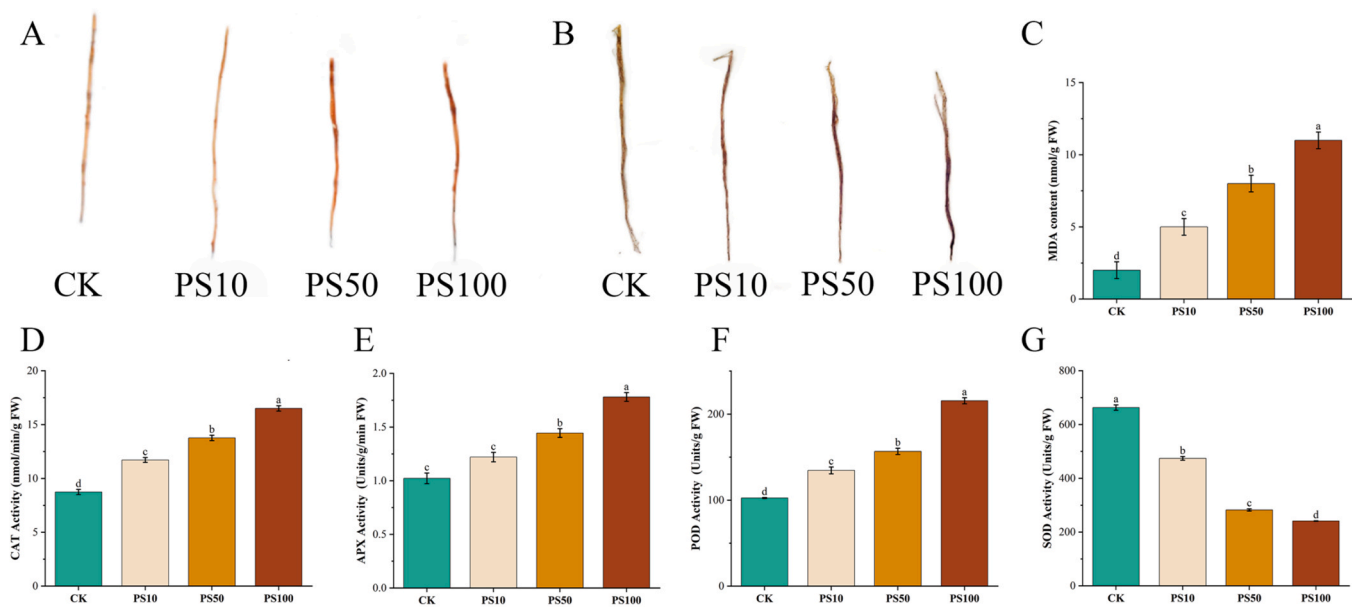


Fig. 3. The effect of different PS-NPs concentrations on antioxidant enzyme. (A) DAB; (B) NBT; (C) MDA content; (D) CAT activity; (E) APX activity; (F) POD activity; (G) SOD activity.

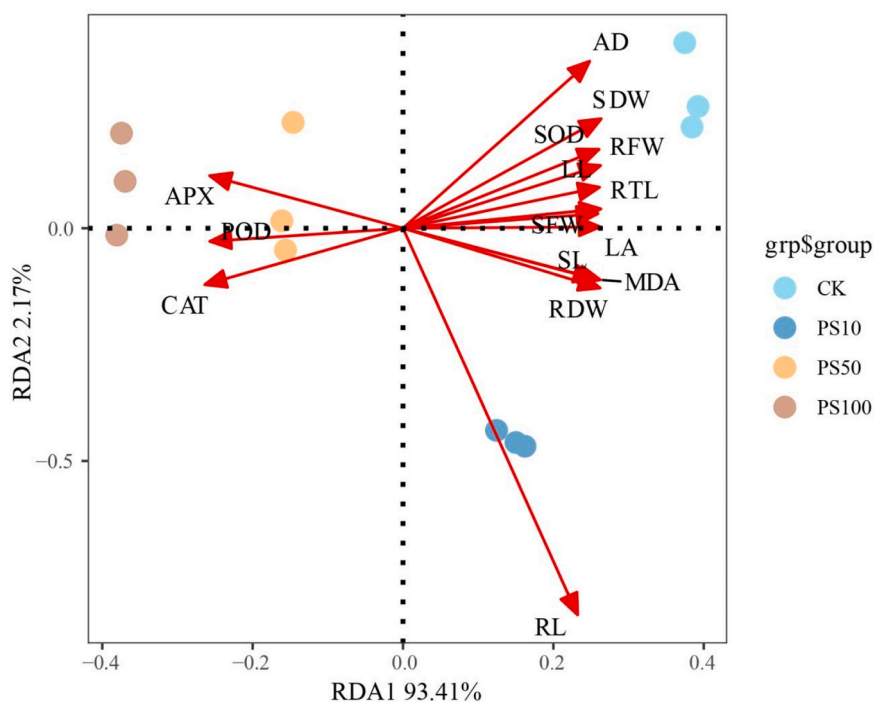


Fig. 4. Redundancy analysis (RDA): shows the scores of seedling growth parameters and antioxidant capacity.

PS50, PS100) to CK, revealing differences between the treatment groups. The PS10 VS CK, PS50 VS CK, and PS100 VS CK groups showed significant differences in "phenylpropanoid biosynthesis" and "plant hormone signaling". These differences suggest that as the intensity of PS-NPs treatment increases, the organism's metabolic responses and regulatory mechanisms also change (Fig. 7A-C).

3.6. Root metabolic analysis with PS-NPs exposure

A PCA model was constructed from the substances identified in the sample. Among them, the contribution of the PC1 was 47 %, and the

contribution of the PC2 was 16.4 % (Fig. 8A). Significant differences in metabolic data were observed among various treatments. Metabolomic analysis revealed significant changes in metabolite expression under different exposure conditions. Specifically, 720 metabolites were up-regulated and 384 were down-regulated under the CK vs PS10 condition. This change in metabolite expression may be related to the adaptive response of cells to environmental changes (Fig. 8B). Further, 674 metabolites were upregulated in CK vs PS50, although the number of down-regulated metabolites was 365 (Fig. 8C). Finally, 1125 metabolites were upregulated and 352 metabolites downregulated in CK vs PS100, suggesting that the changes in these metabolites may reflect the

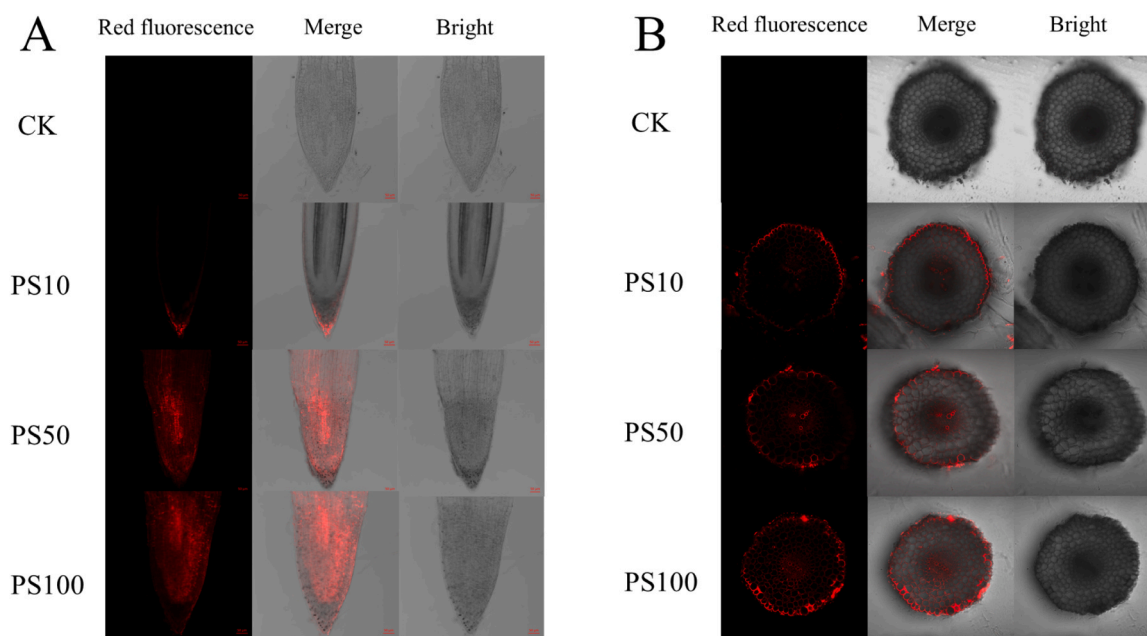


Fig. 5. Confocal image tobacco root tips with fluorescently labeled PS-NPs microspheres. (A) Apex; (B) Transverse.

adjustment of energy metabolism, signaling and biosynthesis pathways in cells under different conditions, providing important clues for in-depth understanding of cellular metabolic regulation mechanisms (Fig. 8D). Code for PS10 vs CK, PS50 vs CK, and PS100 vs CK, the differential metabolites enriched in PS10 VS CK, PS50 VS CK, and PS100 VS CK groups were mainly in "phenylpropanoid biosynthesis" and "plant hormone signaling". (Fig. 9A-C).

3.7. Mining of key genes of tobacco hormones induced by PS-NPs based on WGCNA

To delve deeper into the principal genes that PS-NPs might trigger for plant proliferation, Weighted Gene Co-expression Network Analysis (WGCNA) was frequently employed to investigate the relationship between growth, physiological traits, and key genes. The scale-free topology model's fit curve was observed to be smooth, and the soft threshold power was determined to be $\beta = 6$ (refer to Fig. 10A). Genes with high correlation were grouped into modules, indicating a strong correlation among genes within the same group. The analysis identified a total of 12 distinct modules (Fig. 10B). Notably, the blue module and its associated genes exhibited a significant correlation with POD, SOD, CAT, MDA, and APX (Fig. 10C).

3.8. Co-analysis of lignin content in roots, plant hormone metabolism, and transcription

In roots, compared to CK, 10 mg·L⁻¹ PS-NPs slightly increased the lignin content. However, as the concentration of PS-NPs further increased, a decreasing trend in lignin content was observed. Specifically, at a concentration of 50 mg·L⁻¹, the lignin content decreased by 12.59 %, and most notably at 100 mg·L⁻¹, the inhibition was most significant with a decrease of 16.74 %. These results were generally consistent with the trends in the expression of key genes involved in the lignin synthesis pathway. Through screening and analysis of transcriptome data, we found that the trend of expression of *POD* genes generally decreased as the concentration of PS-NPs treatment increased. Among all the genes, 107770624 and 107828964 exhibited the highest expression levels. Furthermore, their expression peaked under PS10 treatment (Fig. 11B).

As alluded to earlier, KEGG analysis indicated significant enrichment

in "plant hormone signal transduction" among treatments with varying concentrations of PS-NPs. This observation prompted a detailed examination and analysis of the metabolic and transcriptional profiles of two pivotal hormones implicated in lignin biosynthesis. Within the ABA synthesis and signaling cascade, the quantity of β -Carotene, a precursor for ABA production, showed a marked decline with escalating PS-NPs concentrations. The expression of *NCED* was generally elevated compared to the control but also exhibited a downward trend as PS-NPs concentrations increased. Genes associated with the ABA signaling pathway, such as *SnRK2*, *PP2C*, *PYR/PYL*, and *ABF*, all displayed a decreasing pattern (Fig. 11A). Conversely, the ethylene synthesis and signaling pathway was markedly upregulated with rising PS-NPs concentrations. SAM and ACC, crucial metabolites in ethylene biosynthesis, were present at significantly higher levels in all PS-NPs treatments compared to the control. Among the key genes in ethylene synthesis, the expression levels of *SAMS*, *ACS*, *ACO*, and *ETR* were upregulated in response to increasing PS-NPs concentrations. Similarly, genes related to the ethylene signaling pathway also exhibited the same trend, with *MPK6*, *EIN2*, and *ERF1/2* showing increased expression in response to PS-NPs stimulation (Fig. 11C). In addition, auxin, an important hormone that influences lignin synthesis, also exhibited subtle changes under PS-NPs treatment. The specific details are provided in the supplementary data (Fig. S8). A brief summary of these results was: Low concentrations of PS-NPs promoted ABA synthesis, which favor lignin synthesis, while at high concentrations, ethylene dominated and accelerated lignin decomposition.

3.9. Responses between physiological data and transcription and metabolism

These findings were further supported by interactive network analysis, in which ABA, IAA, and ethylene-related enzyme activities are significantly correlated (Fig. 12). This was consistent with their known role in plant signaling. Color-coded correlation plots showed the Pearson correlation coefficients between these key enzymes or metabolites and plant physiological data and enzyme activity. The shades of color of the positive correlation (blue) and negative correlation (red) reflected the strength of the correlation.

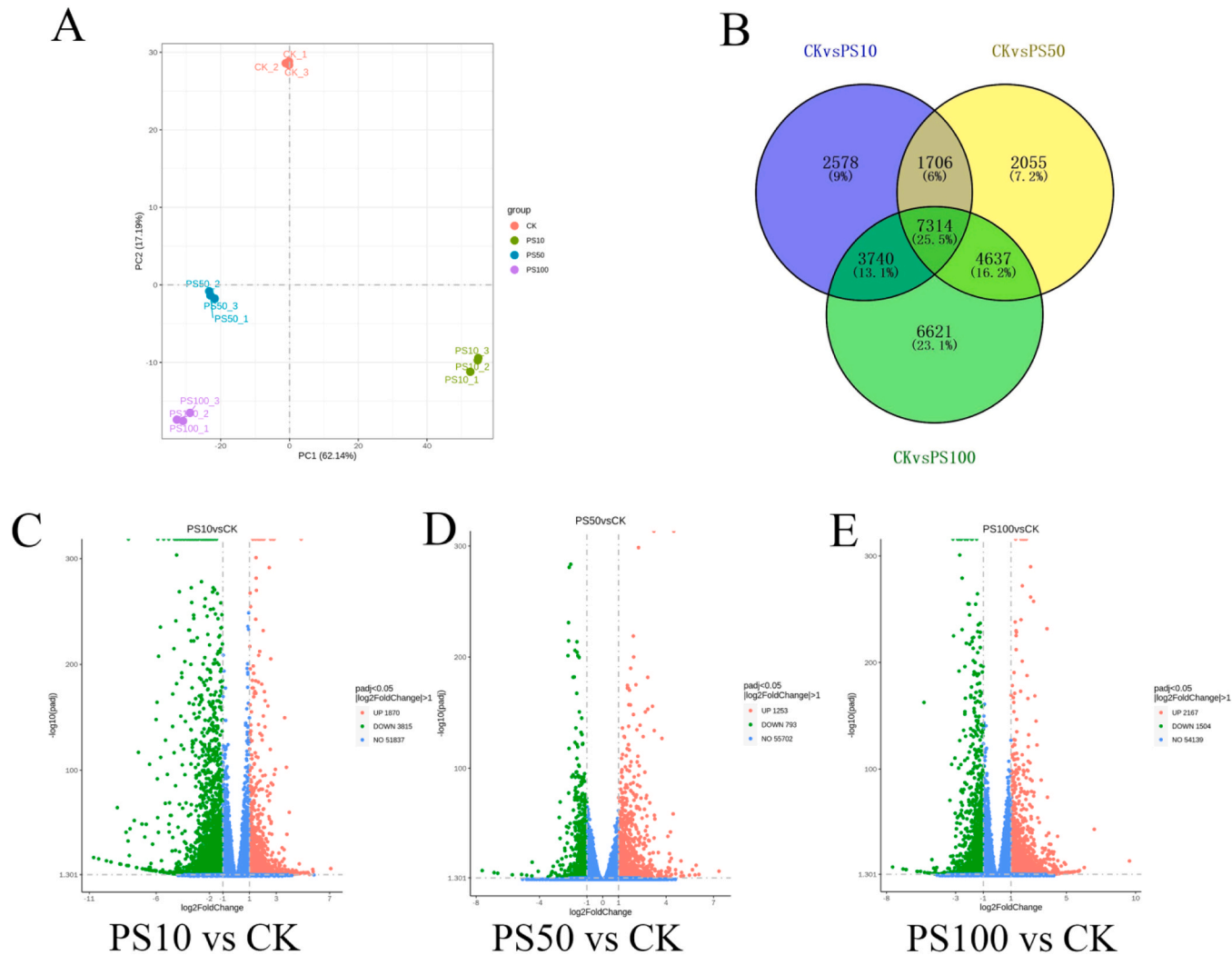


Fig. 6. Identification and enrichment of DAMs in tobacco roots exposed to different concentrations of PS-NPs. (A) PCA score plot; (B) Venn plot of the number of differentially expressed genes; (C, D, and E) Volcano plot of DAMs.

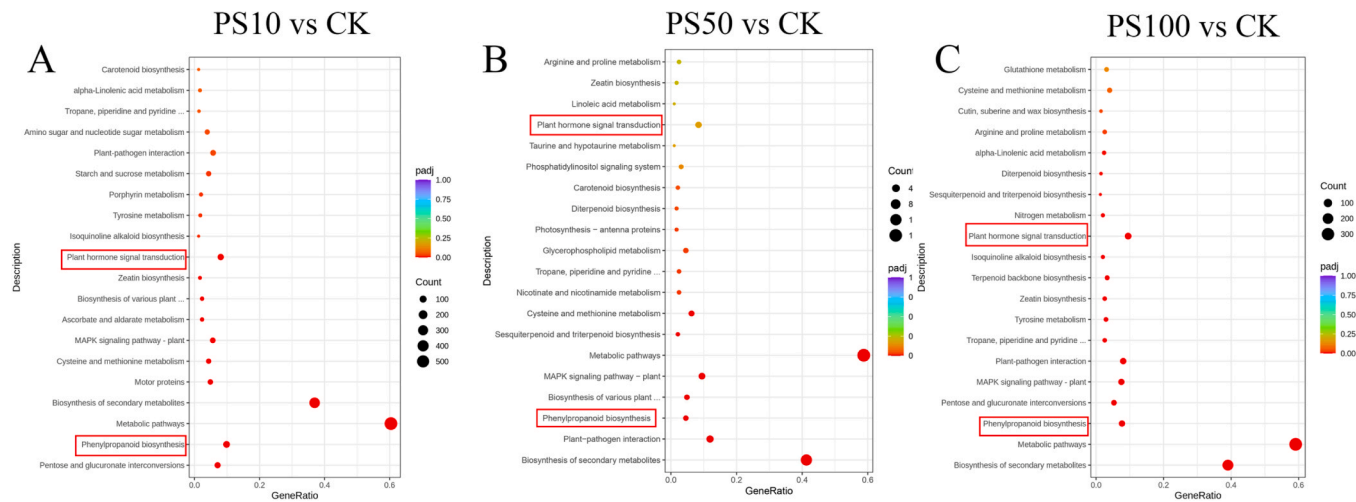


Fig. 7. The top 20 was in the most abundant KEGG pathway (A) PS10 vs CK; (B) PS50 vs CK; (C) PS100 vs CK.

3.10. Partial least squares path modeling analysis

The result indicated that PS-NPs showed negative effects on shoot

biomass and root biomass, with coefficients of -0.5341 and -0.646 , respectively, which may be related to the potential inhibition of plant growth by PS-NPs. There was significant negative correlation between

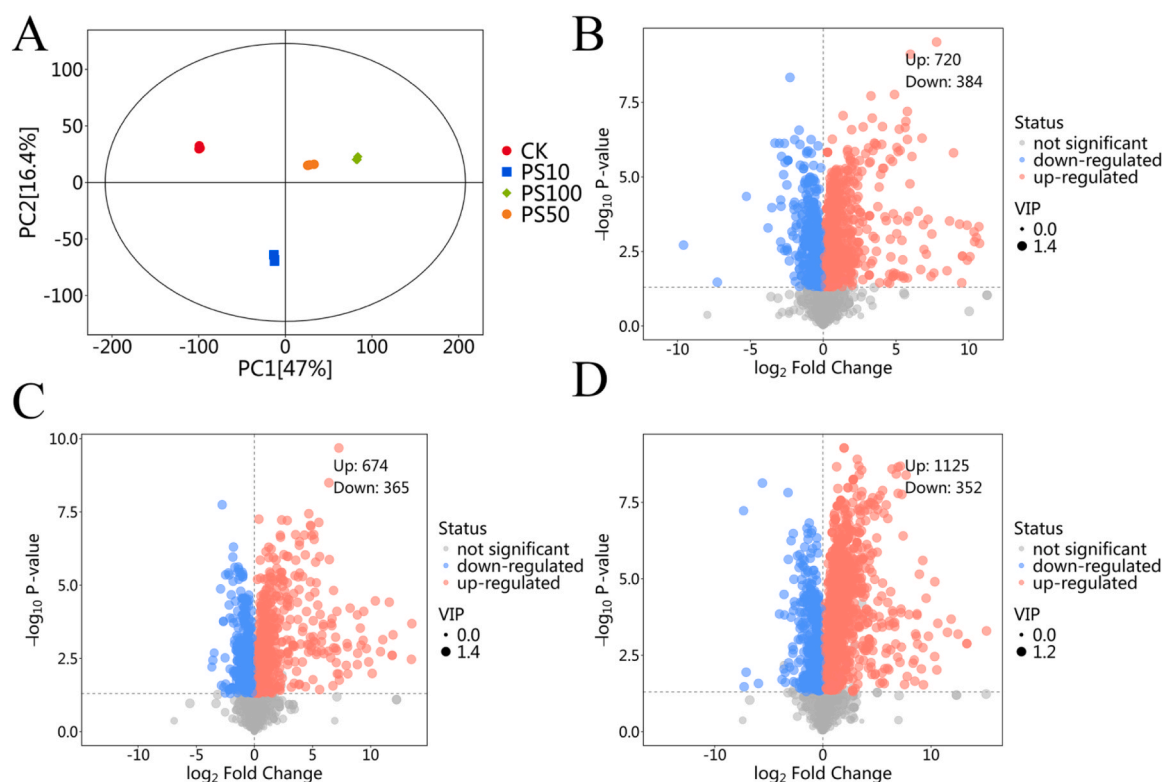


Fig. 8. Expression patterns and volcanic patterns of metabolites in tobacco roots with different concentrations of PS-NPs (A) PCA; (B) CK vs PS10 volcano plot; (C) CK vs PS50 volcano plot; (D) CK vs PS100 volcano plot.

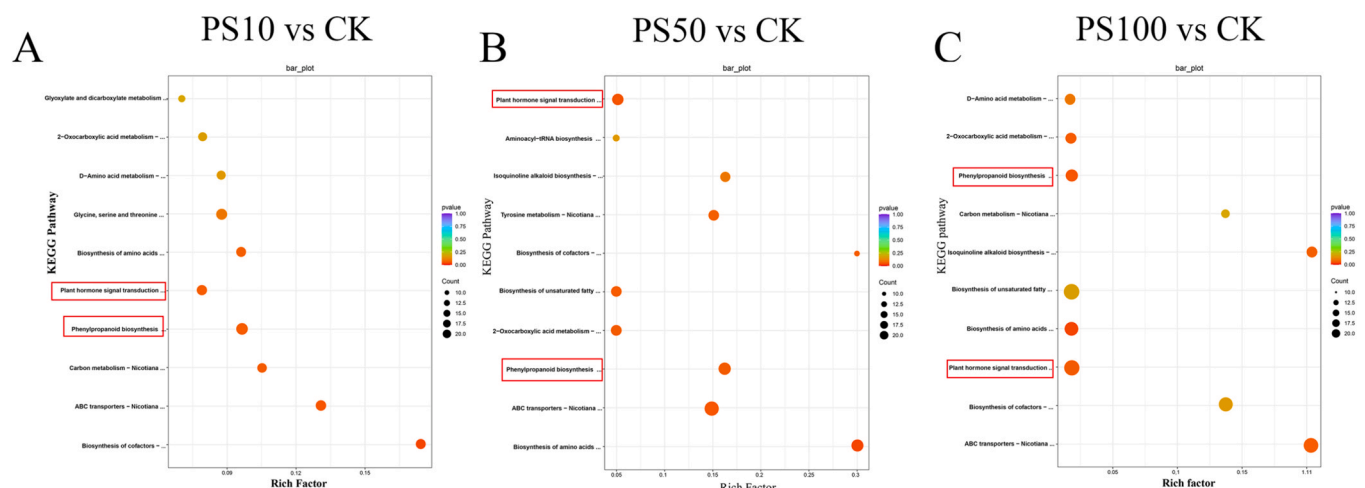


Fig. 9. Effects of different concentrations of PS-NPs on the expression pattern and enrichment pathway of tobacco root metabolites. All KEGG dot (A) PS10 vs CK; (B) PS50vsCK; (C) PS100vsCK.

antioxidants and stem biomass, with a pathway coefficient of -1.2139 , suggesting that despite the increase in antioxidant enzyme activity induced by PS-NPs (0.9703), the growth of the plants still cannot avoid being inhibited by PS-NPs. In addition, the negative correlation between PS-NPs and lignin with coefficient of -0.6547 further suggested that PS-NPs may affect plant structure by reducing lignin content. The positive effect of lignin on shoot biomass, with coefficient of 0.4363 , and on root biomass, with coefficient of 0.3257 , suggested that lignin might play an important role in protecting the plant from PS-NPs toxicity (Fig. 13).

4. Discussion

As human activities escalate, the pollution of global ecosystems by plastic products has become increasingly severe. This issue has generated significant concern, particularly due to the ongoing increase in plastic pollution in freshwater and on land, which represents serious threats to both human health and the environment (Sun and Wang, 2023). Small plastic fragments, amongst others resulting from the degradation of larger debris were classified based on their diameter: MPs ranging from 1 to $5000 \mu\text{m}$, and NPs measuring less than $1 \mu\text{m}$ (Shi, 2023). MPs/NPs have an important inhibitory effect on plant growth, and this inhibitory effect is closely related to particle MPs/NPs

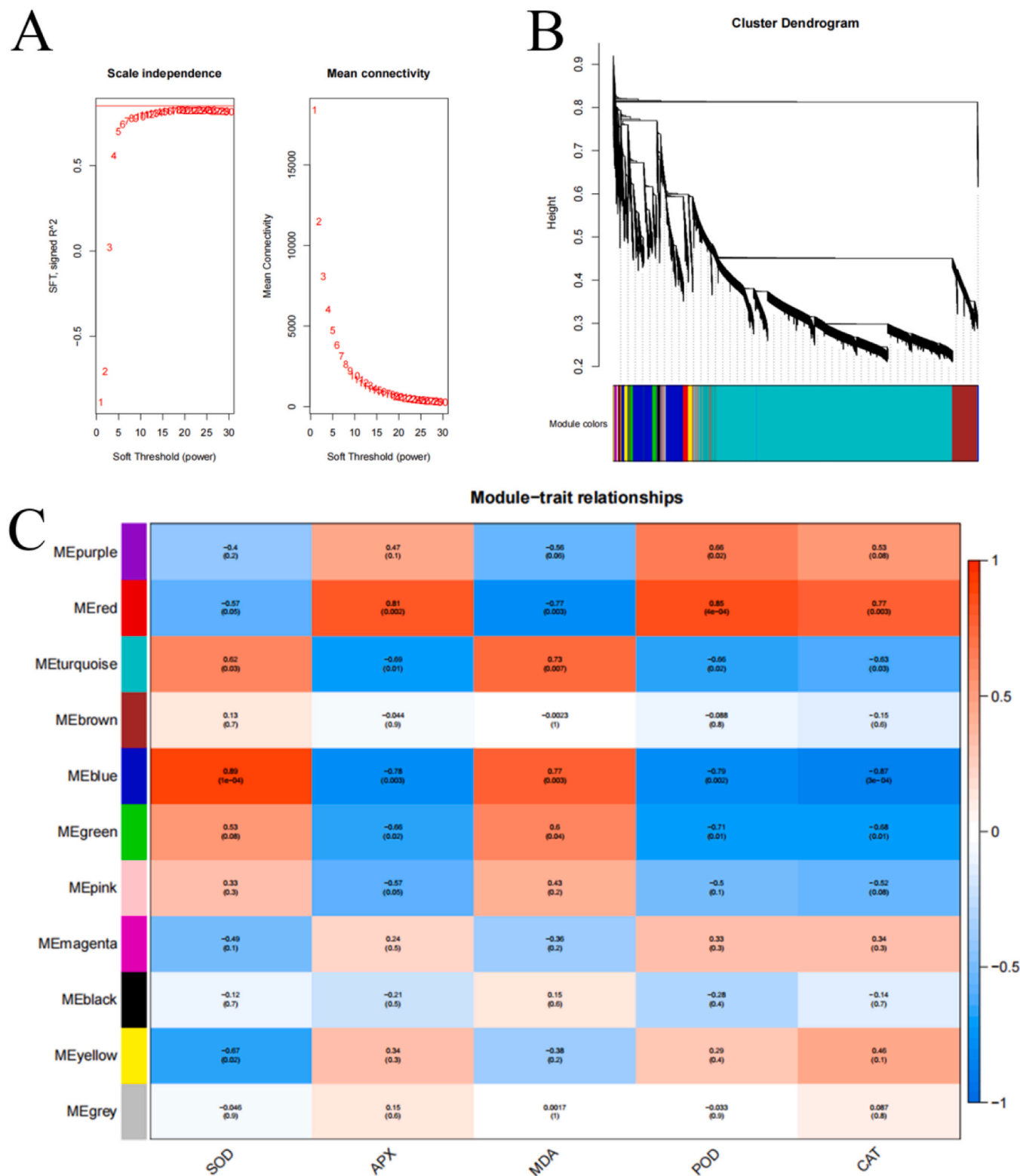


Fig. 10. WGCNA screens root-related marker genes, followed by GO and KEGG analysis of selected marker genes (A) Use soft thresholds for scale-free network analysis; (B) Hierarchical clustering dendrogram of sample gene co-expression in the dataset, with a total of 12 modules identified; (C) Correlation analysis of different modules with tobacco root genes.

properties such as chemical composition, diameter, dose and stress duration (Azeem et al., 2022). Roots are the first part of plants to come in contact with MPs/NPs, and various studies have shown that the amount of MPs/NPs accumulated in roots is much higher than in the aerial parts (Zhou, 2021). Therefore, the effect of MPs/NPs on root

growth and development is the key factor to inhibit plant growth (De Souza Machado et al., 2019). However, the underlying mechanism of inhibition of root growth and the stress response exhibited by the root system by MPs/NPs have not yet been clearly explained.

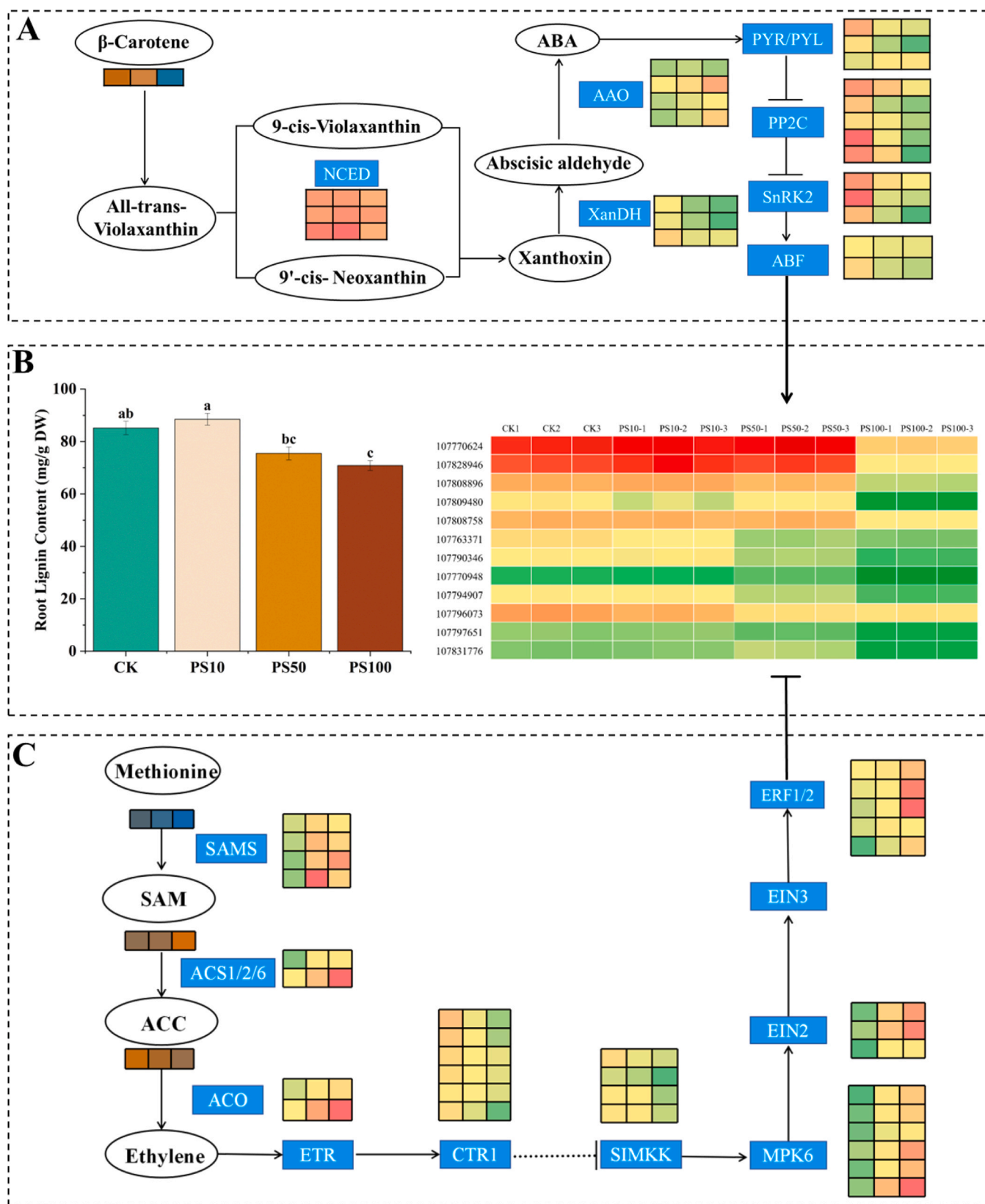


Fig. 11. The relationship between changes in plant hormones and root lignin content under different concentrations of PS-NPs treatment. (A) Expression of DEGs and DEMs in root ABA synthesis and signal transduction; (B) Roots lignin content and the expression of its key biosynthesis genes (PODs) among DEGs; (C) Expression of DEGs and DEMs in root ethylene synthesis and signal transduction. As the concentration of PS-NPs increased, the genes related to ABA signaling that positively regulated lignin synthesis were gradually downregulated, while the ethylene signaling pathway that negatively regulated lignin synthesis was significantly upregulated. Under such conditions, the key genes (PODs) responsible for lignin synthesis in the roots were downregulated in response to the increasing concentration of PS-NPs, leading to a decrease in root lignin content.

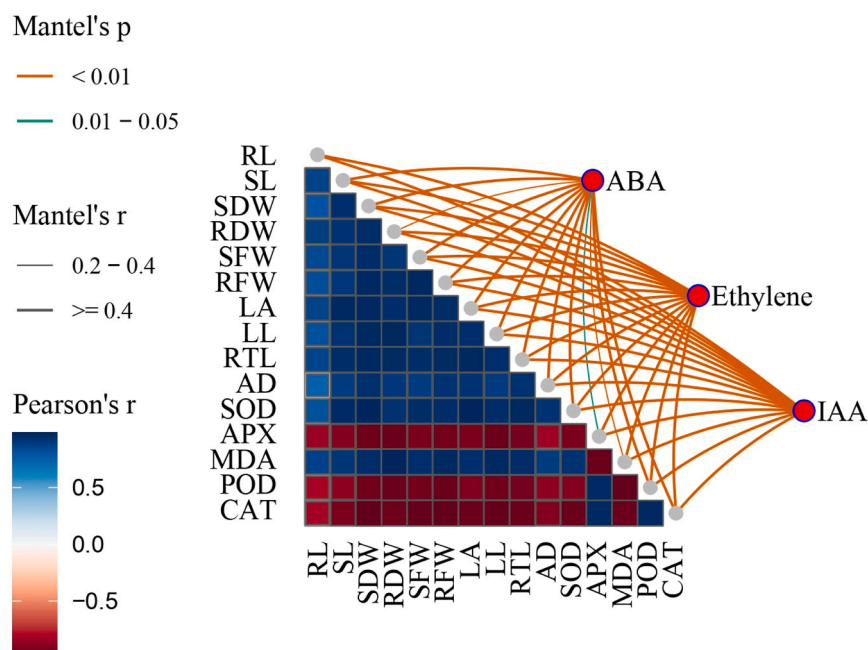


Fig. 12. Correlation analysis diagram showing the Pearson correlation coefficient between variables, color-coded for positive and negative correlation (blue: positive correlation, red: negative correlation), Mantel test results are represented by line color and thickness, orange line for $p < 0.01$, green line for $0.01 \leq p < 0.05$, line thickness for Mantel's r value (fine line: $0.2-0.4$, thick line: ≥ 0.4).

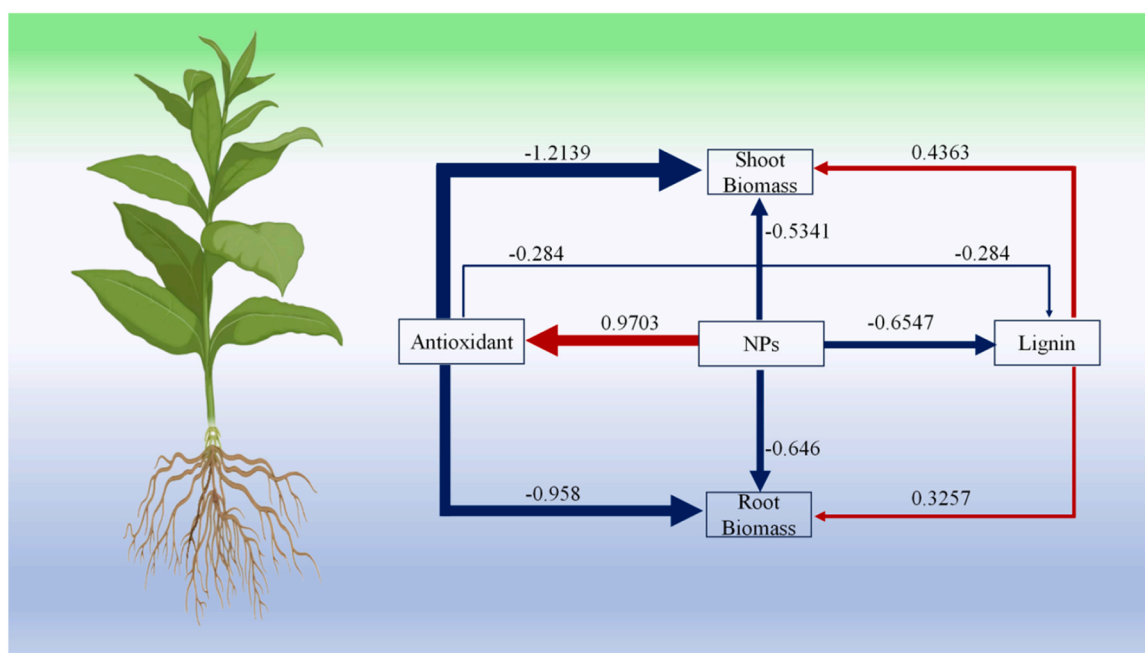


Fig. 13. Results of Partial Least Squares Path Modeling (PLS-PM). The one-way cause-total effect between the five variables is shown as arrows with path coefficients (red and blue arrows indicate positive and negative effects, respectively). The value above the arrow in the model represents the weight of the measured variable.

4.1. Effect of PS-NPs on plant physiological parameters

The results indicated that the growth of tobacco seedlings was significantly inhibited as the concentration of PS-NPs increased. This inhibitory effect on growth became more pronounced with higher PS-NPs concentrations, reaching its peak at $100 \text{ mg}\cdot\text{L}^{-1}$ (Fig. 2). Similar findings were observed in other crops, such as wheat, corn, and soybeans. In wheat, 2 % (w/w) PS led to significant reductions in biomass and root development through decreasing chlorophyll content in wheat leaves, thus affecting photosynthesis efficiency (Gao et al., 2024). In

maize, 1 % (w/w) PP reduced both root and shoot length and decreased chlorophyll a and b content (Martín et al., 2023). Additionally, 5 % (w/w) PE negatively impacted soybean growth, including reductions in biomass, root length, and total uptake area of the root system. Increasing PS concentrations significantly reduced wheat biomass, impaired root growth, and lowered chlorophyll levels. These effects were due to polyvinyl chloride microplastics disrupting key plant processes like photosynthesis and root development (Zhang et al., 2024). Although the underlying mechanism through which MPs/NPs inhibited plant growth had not been fully elucidated, an increasing body of literature

demonstrated that MPs/NPs exerted a damaging effect on the membrane system.

4.2. PS-NPs produced oxidative damage and induced antioxidant enzyme activity change

ROS constitute a group of highly reactive oxygen-containing compounds. These molecules have crucial physiological functions within cells, such as acting in signaling pathways, facilitating cell differentiation, and participating in defense mechanisms (Sies and Jones, 2020). Nevertheless, an overabundance of ROS can cause harm to cellular components, resulting in oxidative stress and impairment of cellular function (Ghosh et al., 2018). Over the past few years, numerous investigations have shown that MPs/NPs can induce oxidative stress by elevating ROS levels within biological systems. In particular, the superoxide anion ($O_2^{\cdot-}$) and hydroxyl radical ($\cdot OH$), which are produced through the photodegradation of microplastics, intensify oxidative stress and subsequently boost the generation of ROS in the roots of plants. (Duan et al., 2022). PS substantially increased the concentration of ROS in the root cells of wheat, leading to oxidative stress and cellular damage (Bao et al., 2022). Additionally, studies have demonstrated that the levels of ROS in lettuce leaves significantly rose when exposed to PE, coinciding with noticeable changes in the plant's antioxidant defense mechanisms (Song, 2020). Our experimental findings indicated that the accumulation of ROS and the corresponding fluorescence intensity in seedlings were elevated with escalating exposure to PS-NPs (Fig. 3A-B).

As stress intensity increased, plants minimized the accumulation of ROS by enhancing the antioxidant enzymes activity to maintain the redox balance in cells. Increase of antioxidant enzyme activity was also found in cucumber (Li et al., 2020) and pak choi (Yu et al., 2022). However, it should be noted that even with increased antioxidant activity, high concentrations of MPs/NPs could continuously lead to ROS accumulation and oxidative damage in plants (Ma, 2022).

4.3. PS-NPs Modulating Plant Hormone Balance

Plant hormones is the key factor in the growth and development processes of plants. Under normal growth conditions, auxin plays a major role, while the levels of stress response hormones such as ABA and ethylene were relatively low (Waadt et al., 2022). However, when plants were subjected to a stressor, the balance of the various hormones in the plants was disrupted, enhancing their ability to adapt to challenging conditions. A typical characteristic was a decrease of the auxin content (Shani et al., 2017). In contrast, ABA and ethylene were upregulated to regulate the physiological response of plants and enhance their adaptability to adverse environmental conditions for instance drought, salt, temperature stress, pests and diseases (Zhang et al., 2020; Yadav et al., 2023).

In order to clarify the effect of PS-NPs on the hormone signaling pathway, the transcriptome and metabolome characterizations were conducted for each of the PS-NPs exposure doses. "Plant hormone signal transduction" along with "amino acid biosynthesis", "carbon metabolism" and "ABC transporter" were observed to be affected in the different doses of the PS-NPs treatment groups. In particular, the KEGG results indicated that the "plant hormone signaling pathway" was significantly enriched in the comparisons between different treatments. This suggested that PS-NPs treatment may interfere with plant hormone signaling pathways, thereby inducing plant responses to environmental stresses.

ABA was one of the most important stress-responsive hormones, particularly under water stress conditions, where it effectively regulated stomatal closure, which in turn significantly enhanced the water use efficiency of plants (Munemasa et al., 2015). Recent molecular biology studies shown that ABA could enhance plant stress tolerance by regulating gene expression. For example, under water stress, ABA regulated aquaporin expression in roots to promote water absorption (Liu et al.,

2024). ABA regulated plant growth primarily through two factors: the synthesis of ABA and its signaling pathways. During the synthesis of ABA, NCED acted as a key enzyme, and its expression levels directly influenced ABA content (Cutler and Krochko, 1999). The results of this experiment indicated that when the roots were exposed to PS-NPs, the expression level of *NtNCED* was significantly upregulated compared to the CK. However, as the concentration of PS-NPs increased, the expression level declined (Fig. 11A). In the ABA signaling pathway, PYR/PYL functions as an ABA receptor, with PP2C and SnRK2 serving as regulatory components. In the presence of ABA, the formation of the PYR/PYL-PP2C complex inhibited PP2C activity, which subsequently activated SnRK2, thereby targeting ABA-responsive genes (Lin et al., 2021). In this experiment, the expression of PP2C and SnRK2 was upregulated at low concentrations but downregulated at high concentrations, negatively affecting ABA signal transduction (Lin et al., 2021).

Under adverse conditions, plants often produce large amounts of ethylene. This helps plants to adapt to unfavorable environments. More importantly, stress conditions altered the allocation of energy in the plant as represented by reduced growth and accelerated reproductive development (Kazan, 2015). In the synthesis of ethylene, S-adenosylmethionine (SAM) was converted to 1-aminocyclopropane-1-carboxylic acid by ACS, which was the rate-limiting enzyme in the process (Lin et al., 2009). In this experiment, the metabolomic results indicated that after treatment with PS-NPs, the expression of SAM in plants significantly increased, leading to a decrease in methionine content and a notable rise in SAM levels. This, in turn, promoted the synthesis of ACC under the action of ACS. In the signaling pathway, aside from the negatively acting *SIMKK*, other genes (e.g., *ETR*, *CTR1*, *EIN2*, *EIN3/ELL*, and *ERF1*) related to the signaling pathways were significantly upregulated, and the expression levels of these genes increased with increasing concentrations of PS-NPs.

4.4. Multi-omics analysis shows the hormones balance to control lignin content in the cell wall

Until now, almost all investigations have confirmed that the primary pathway for MPs/NPs transport in roots is through the apoplast continuum, and physical and mechanical barriers such as the cell wall and the Casparian strip are the significant factors inhibiting the transport of MPs/NPs (Rillig et al., 2019). As a crucial ingredient of the cell wall, lignin can strengthen the root cell wall, reduce the transport of inorganic ionic, and significantly improve the resistance of plants to salt and heavy metals (Cesarino, 2019). A number of reviews explored the various factors influencing lignin synthesis, including plant hormones, environmental stress, gene expression, and metabolic pathways. Hormones such as ABA, ethylene play a crucial role in lignin accumulation (Zhao et al., 2011).

Under a range of stress conditions, ABA can enhance the lignin production genes expression, which thickens cell walls and restricts the uptake and translocation of heavy metals. In *Arabidopsis*, the subnetwork analysis revealed that ABA is linked to nine transcription factors MYB that play key role in the biosynthesis of suberin and lignin within the common sky root system (Xu et al., 2022). Especially under stress conditions, ABA induced lignin participated in plant stress resistance. In maize, *ZmHLH105* activated *ZmNCED1/2* expression to increase endogenous ABA levels, which subsequently enhanced the lignin content to reduce the Cd^{2+} uptake and transportation through the apoplastic space (Meng et al., 2024). Similar results were also found in different species under drought (Lin et al., 2021), salt (Szypulska et al., 2017), and cold stress (Feng et al., 2019).

In contrast to the effects of ABA, ethylene typically facilitates a reduction in lignin levels (Gaddam et al., 2022; Yang et al., 2023; Zhao et al., 2023b). When ACC, a precursor to ethylene, was applied to *Arabidopsis*, it led to a notable decrease in root suberization. Conversely, mutants with impaired ethylene signaling exhibited increased suberization (Barberon et al., 2016). Two independent homozygous

PagERF81 mutant lines exhibited increased lignin deposition in cell walls, whereas lignin content significantly decreased in overexpression plants. This result indicated the transcription factors ERF in the ethylene signaling pathway were negatively correlated with cellular lignin production (Zhao et al., 2023b). It has been clarified that ethylene functions upstream of the miR397b/miR857-laccase module, inhibiting lignin biosynthesis by directly stimulating the expression of both miRNAs (Gaddam et al., 2022).

Notably, auxin, another key regulator of lignification, also exhibited subtle yet notable changes under PS-NPs stress. Previous studies have shown that auxin can promote lignin synthesis by upregulating the expression of peroxidase (POD) and cinnamate 4-hydroxylase (C4H) genes in the phenylpropanoid pathway (Zhao et al., 2011). However, in our transcriptomic data, auxin synthesis and responsive genes showed moderate downregulation at high PS-NPs concentrations (Fig. S8), which may not be the main factor of lignin biosynthesis under PS-NPs stress. However, this effect was overshadowed by the dominant roles of ABA and ethylene in our experimental system, highlighting the complexity of hormone crosstalk during PS-NPs stress.

The lignin content is the result of a dynamic balance among these hormones (Zhao and Dixon, 2011). In the present study, the content of lignin first enhanced and then declined upon with the treatment of PS-NPs. Through a combined analysis of transcription and metabolism, we hypothesized that the dynamic changes in ABA and ethylene were responsible for this phenomenon. At low concentrations, the gene expression levels and metabolite levels involved in ABA synthesis and signal transduction are higher than those at high concentrations. In contrast, ethylene exhibited an opposite trend, with the genes related to synthesis, particularly those in the signaling pathway, being significantly upregulated as the concentration of PS-NPs increased. In other words, at low concentrations, ABA had taken the lead, promoting lignin synthesis, while at higher concentrations, ethylene had replaced ABA as the dominant hormone, facilitating lignin degradation (Figs. 11 and 12).

5. Conclusion

MPs/NPs were absorbed by tobacco root systems and translocated to the leaves, potentially presenting substantial health hazards when the tobacco is smoked. It is crucial to understand the processes of MPs/NPs accumulation and their toxic effects. In our study, the enhancement of PS-NPs concentration led to significant increase in PS-NPs accumulation in tobacco roots, which in turn resulted in stunted tobacco growth. This reduction in growth was closely associated with the increased presence of ROS within the plant. To combat the toxicity of PS-NPs, plant roots enhanced their resistance by regulating metabolic activities. The increase in antioxidant enzyme activity helped to reduce the accumulation of ROS. More importantly, a combined analysis of transcription and metabolism identified key factors in hormone regulation that enhanced root resilience. Lignin played a crucial role in strengthening the physical barriers of the root exodermis and was shown to be vital in mitigating the effects of harmful substances. At lower concentrations, there was a notable increase in the lignin levels within the roots, which correlated with the activation of the ABA signaling pathway. However, with further increases in the concentration of PS-NPs, the augmentation of the ethylene signaling pathway led to a decrease in lignin content, potentially playing a pivotal role in the suppression of plant growth at elevated concentrations. Collectively, this research not only offered a comprehensive insight into how PS-NPs impact tobacco growth but also shed light on the mechanisms that govern tobacco's response to PS-NPs exposure.

CRediT authorship contribution statement

Peng Liu: Writing – review & editing, Supervision, Project administration, Funding acquisition. **Long Yang:** Writing – review & editing, Funding acquisition. **Xiaodong Sun:** Software, Methodology. **Wenwen**

Li: Writing – review & editing. **Jingrui Chen:** Visualization. **Willie J.G. M. Peijnenburg:** Writing – review & editing, Methodology. **Tao Jia:** Writing – original draft, Visualization, Investigation, Data curation.

Declaration of Competing Interest

The authors declare that they have no known competing financial interests or personal relationships that could have appeared to influence the work reported in this paper.

Acknowledgements

The Foundation of the Modern Agricultural Technology Industry System in Shandong Province (SDAIT-25-01 and SDAIT-25-07) provided funding for this research.

Appendix A. Supporting information

Supplementary data associated with this article can be found in the online version at doi:10.1016/j.indcrop.2025.121356.

Data availability

Data will be made available on request.

References

- Ali, I., Cheng, Q., Ding, T., Yiguang, Q., Yuechao, Z., Sun, H., Peng, C., Naz, I., Li, J., Liu, J., 2021. Micro- and nanoplastics in the environment: occurrence, detection, characterization and toxicity – a critical review. *J. Clean. Prod.* 313, 127863. <https://doi.org/10.1016/j.jclepro.2021.127863>.
- Arif, Y., Mir, A.R., Zieliński, P., Hayat, S., Bajguz, A., 2024. Microplastics and nanoplastics: source, behavior, remediation, and multi-level environmental impact. *J. Environ. Manag.* 356, 120618. <https://doi.org/10.1016/j.jenvman.2024.120618>.
- Azeem, I., Adeel, M., Ahmad, M.A., Shakoar, N., Zain, M., Yousef, N., Yinghai, Z., Azeem, K., Zhou, P., White, J.C., Ming, X., Rui, Y., 2022. Microplastic and nanoplastic interactions with plant species: trends, meta-analysis, and perspectives. *Environ. Sci.* <https://doi.org/10.1021/acs.estlett.2c00107>.
- Bao, Y., Pan, C., Li, D., Guo, A., Dai, F., 2022. Stress response to oxytetracycline and microplastic-polyethylene in wheat (*Triticum aestivum* L.) during seed germination and seedling growth stages. *Sci. Total Environ.* 806, 150553. <https://doi.org/10.1016/j.scitotenv.2021.150553>.
- Barberon, M., Vermeer, J.E.M., De Bellis, D., Wang, P., Naseer, S., Andersen, T.G., Humbel, B.M., Nawrath, C., Takano, J., Salt, D.E., Geldner, N., 2016. Adaptation of root function by nutrient-induced plasticity of endodermal differentiation. *Cell* 164 (3), 447–459. <https://doi.org/10.1016/j.cell.2015.12.021>.
- Cesarino, I., 2019. Structural features and regulation of lignin deposited upon biotic and abiotic stresses. *Curr. Opin. Biotechnol.* 56, 209–214. <https://doi.org/10.1016/j.copbio.2018.12.012>.
- Cutler, A.J., Krochko, J.E., 1999. Formation and breakdown of ABA. *Trends Plant Sci.* 4 (12), 472–478. [https://doi.org/10.1016/S1360-1385\(99\)01497-1](https://doi.org/10.1016/S1360-1385(99)01497-1).
- Da Costa, J.P., Santos, P.S.M., Duarte, A.C., Rocha-Santos, T., 2016. Nano)plastics in the environment – Sources, fates and effects. *Sci. Total Environ.* 566–567, 15–26. <https://doi.org/10.1016/j.scitotenv.2016.05.041>.
- Dar, N.A., Amin, I., Wani, W., Wani, S.A., Shikari, A.B., Wani, S.H., Masoodi, K.Z., 2017. Abscissic acid: a key regulator of abiotic stress tolerance in plants. *Plant Gene* 11, 106–111. <https://doi.org/10.1016/j.plgene.2017.07.003>.
- De Souza Machado, A.A., Lau, C.W., Kloas, W., Bergmann, J., Bachelier, J.B., Faltin, E., Becker, R., Görlich, A.S., Rillig, M.C., 2019. Microplastics can change soil properties and affect plant performance. *Environ. Sci. Technol.* 53 (10), 6044–6052. <https://doi.org/10.1021/acs.est.9b01339>.
- Duan, J., Li, Y., Gao, J., Cao, R., Shang, E., Zhang, W., 2022. ROS-mediated photoaging pathways of nano- and micro-plastic particles under UV irradiation. *Water Res.* 216, 118320. <https://doi.org/10.1016/j.watres.2022.118320>.
- Feng, X., Xu, Y., Peng, L., Yu, X., Zhao, Q., Feng, S., Zhao, Z., Li, F., Hu, B., 2019. *TaEXP7-B*, a β -expansin gene involved in low-temperature stress and abscisic acid responses, promotes growth and cold resistance in *Arabidopsis thaliana*. *J. Plant Physiol.* 240, 153004. <https://doi.org/10.1016/j.jplph.2019.153004>.
- Gaddam, S.R., Bhatia, C., Gautam, H., Pathak, P.K., Sharma, A., Saxena, G., Trivedi, P.K., 2022. Ethylene regulates miRNA-mediated lignin biosynthesis and leaf serration in *Arabidopsis thaliana*. *Biochem. Biophys. Res. Commun.* 605, 51–55. <https://doi.org/10.1016/j.bbrc.2022.03.037>.
- Gan, Q., Cui, J., Jin, B., 2023. Environmental microplastics: classification, sources, fates, and effects on plants. *Chemosphere* 313, 137559. <https://doi.org/10.1016/j.chemosphere.2022.137559>.
- Ghosh, N., Das, A., Chaffee, S., Roy, S., & Sen, C.K. (2018). Reactive Oxygen Species, Oxidative Damage and Cell Death. Immunity and Inflammation in Health and Disease (45–55). Elsevier. <https://doi.org/10.1016/B978-0-12-805417-8.00004-4>.

- Gao, W., Wu, D., Zhang, D., Geng, Z., Tong, M., Duan, Y., Xia, W., Chu, J., Yao, X., 2024. Comparative analysis of the effects of microplastics and nitrogen on maize and wheat: Growth, redox homeostasis, photosynthesis, and AsA-GSH cycle. *Sci. Total Environ.* 932, 172555. <https://doi.org/10.1016/j.scitotenv.2024.172555>.
- Hua, Z., Ma, S., Ouyang, Z., Liu, P., Qiang, H., Guo, X., 2023. The review of nanoplastics in plants: Detection, analysis, uptake, migration and risk. *TrAC Trend. Anal. Chem.* 158, 116889. <https://doi.org/10.1016/j.trac.2022.116889>.
- Huang, S., Huang, X., Bi, R., Guo, Q., Yu, X., Zeng, Q., Huang, Z., Liu, T., Wu, H., Chen, Y., Xu, J., Wu, Y., Guo, P., 2022. Detection and analysis of microplastics in human sputum. *Environ. Sci. Technol.* <https://doi.org/10.1021/acs.est.1c03859>.
- Kazan, K., 2015. Diverse roles of jasmonates and ethylene in abiotic stress tolerance. *Trends Plant Sci.* 20 (4), 219–229. <https://doi.org/10.1016/j.tplants.2015.02.001>.
- Lee, Y., Cho, S., Park, K., Kim, T., Kim, J., Ryu, D.-Y., Hong, J., 2023. Potential lifetime effects caused by cellular uptake of nanoplastics: a review. *Environ. Pollut.* 329, 121668. <https://doi.org/10.1016/j.envpol.2023.121668>.
- Li, Y., Chen, L., Zhou, N., Chen, Y., Ling, Z., Xiang, P., 2024. Microplastics in the human body: a comprehensive review of exposure, distribution, migration mechanisms, and toxicity. *Sci. Total Environ.* 946, 174215. <https://doi.org/10.1016/j.scitotenv.2024.174215>.
- Li, Z., Li, R., Li, Q., Zhou, J., Wang, G., 2020. Physiological response of cucumber (*Cucumis sativus* L.) leaves to polystyrene nanoplastics pollution. *Chemosphere* 255, 127041. <https://doi.org/10.1016/j.chemosphere.2020.127041>.
- Lin, Z., Zhong, S., Grierson, D., 2009. Recent advances in ethylene research. *J. Exp. Bot.* 60 (12), 3311–3336. <https://doi.org/10.1093/jxb/erp204>.
- Lin, Z., Li, Y., Wang, Y., Liu, X., Ma, L., Zhang, Z., Mu, C., Zhang, Y., Peng, L., Xie, S., Song, C.-P., Shi, H., Zhu, J.-K., Wang, P., 2021. Initiation and amplification of SnRK2 activation in abscisic acid signaling. *Nat. Commun.* 12 (1), 2456. <https://doi.org/10.1038/s41467-021-22812-x>.
- Liu, C., Yu, H., Rao, X., Li, L., Dixon, R.A., 2021a. Abscisic acid regulates secondary cell-wall formation and lignin deposition in *Arabidopsis thaliana* through phosphorylation of NST1. *Proc. Natl. Acad. Sci.* 118 (5), e2010911118. <https://doi.org/10.1073/pnas.2010911118>.
- Liu, Z., Yan, J., Wang, D., Ahmad, P., Qin, M., Li, R., Ali, B., Sonah, H., Deshmukh, R., Yadav, K.K., El-Sheikh, M.A., Zhang, L., Liu, P., 2024. Silicon improves salt resistance by enhancing ABA biosynthesis and aquaporin expression in *Nicotiana tabacum* L. *Plant Physiol. Biochem.* 215, 108977. <https://doi.org/10.1016/j.plaphy.2024.108977>.
- Lu, W., Li, X., Wang, S., Tu, C., Qiu, L., Zhang, H., Zhong, C., Li, S., Liu, Y., Liu, J., Zhou, Y., 2023. New evidence of microplastics in the lower respiratory tract: inhalation through smoking. *Environ. Sci. Technol.* 57 (23), 8496–8505. <https://doi.org/10.1021/acs.est.3c00716>.
- Ma, J., 2022. Effects of microplastics on growth and metabolism of rice (*Oryza sativa* L.). *Chemosphere* 307, 135749. <https://doi.org/10.1016/j.chemosphere.2022.135749>.
- Meng, Y., Li, M., Guo, Z., Chen, J., Wu, J., Xia, Z., 2024. The transcription factor ZmbHLH105 confers cadmium tolerance by promoting abscisic acid biosynthesis in maize. *J. Hazard. Mater.* 480, 135826. <https://doi.org/10.1016/j.jhazmat.2024.135826>.
- Munemasa, S., Hauser, F., Park, J., Waadt, R., Brandt, B., Schroeder, J.I., 2015. Mechanisms of abscisic acid-mediated control of stomatal aperture. *Curr. Opin. Plant Biol.* 28, 154–162. <https://doi.org/10.1016/j.pbi.2015.10.010>.
- Ogawara, T., Higashi, K., Kamada, H., Ezura, H., 2003. Ethylene advances the transition from vegetative growth to flowering in *Arabidopsis thaliana*. *J. plant physiol.* 160 (11), 1335–1340. <https://doi.org/10.1078/0176-1617-01129>.
- Ramos-González, E.J., Bitzer-Quintero, O.K., Ortiz, G., Hernández-Cruz, J.J., Ramírez-Jirano, L.J., 2024. Relationship between inflammation and oxidative stress and its effect on multiple sclerosis. *Neuro. ía* 39 (3), 292–301. <https://doi.org/10.1016/j.nrl.2021.10.003>.
- Rillig, M.C., Lehmann, A., De Souza Machado, A.A., Yang, G., 2019. Microplastic effects on plants. *N. Phytol.* 223 (3), 1066–1070. <https://doi.org/10.1111/nph.15794>.
- Riseh, R.S., Vazvani, M.G., Vatankhah, M., Kennedy, J.F., 2024. Chitin-induced disease resistance in plants: A review. *Int. J. Biol. Macromol.* 131105. <https://doi.org/10.1016/j.ijbiomac.2024.131105>.
- Schreiber, L., Hartmann, K., Skrabbs, M., Zeier, J., 1999. Apoplastic barriers in roots: chemical composition of endodermal and hypodermal cell walls. *J. Exp. Bot.* 50 (337), 1267–1280. <https://doi.org/10.1093/jxb/50.337.1267>.
- Shani, E., Salehin, M., Zhang, Y., Sanchez, S.E., Doherty, C., Wang, R., Mangado, C.C., Song, L., Tal, I., Pisanty, O., Ecker, J.R., Kay, S.A., Pruneda-Paz, J., Estelle, M., 2017. Plant stress tolerance requires auxin-sensitive Aux/IAA transcriptional repressors. *Curr. Biol.* 27 (3), 437–444. <https://doi.org/10.1016/j.cub.2016.12.016>.
- Shi, H., 2023. Small plastic fragments: a bridge between large plastic debris and micro- & nano-plastics. *Trends Anal. Chem.* <https://doi.org/10.1016/j.trac.2023.117308>.
- Sies, H., Jones, D.P., 2020. Reactive oxygen species (ROS) as pleiotropic physiological signalling agents. *Nat. Rev. Mol. Cell Biol.* 21 (7), 363–383. <https://doi.org/10.1038/s41580-020-0230-3>.
- Song, J., 2020. Nutritional quality, mineral and antioxidant content in lettuce affected by interaction of light intensity and nutrient solution concentration. *Sci. Rep.* 10 (1), 2796. <https://doi.org/10.1038/s41598-020-59574-3>.
- Sun, A., Wang, W.X., 2023. Human exposure to microplastics and its associated health risks. *Environ. Health* 1 (3), 139–149. <https://doi.org/10.1021/envhealth.3c00053>.
- Szypulska, E., Jankowski, K., Weidner, S., 2017. ABA pretreatment can limit salinity-induced proteome changes in growing barley sprouts. *Acta Physiol. Plant.* 39 (8), 190. <https://doi.org/10.1007/s11738-017-2490-x>.
- Torres, C.A., Azocar, C., Ramos, P., Pérez-Díaz, R., Sepúlveda, G., Moya-León, M.A., 2020. Photooxidative stress activates a complex multigenic response integrating the phenylpropanoid pathway and ethylene, leading to lignin accumulation in apple (*Malus domestica* Borkh.) fruit. *Hortic. Res.* 7. <https://doi.org/10.1038/s41438-020-0244-1>.
- Waadt, R., Seller, C.A., Hsu, P.K., Takahashi, Y., Munemasa, S., Schroeder, J.I., 2022. Plant hormone regulation of abiotic stress responses. *Nat. Rev. Mol. Cell Biol.* 23 (10), 680–694. <https://doi.org/10.1038/s41580-022-00479-6>.
- Wu, X., Yan, J., Qin, M., Li, R., Jia, T., Liu, Z., Ahmad, P., El-Sheikh, M.A., Yadav, K.K., Rodríguez-Díaz, J.M., Zhang, L., Liu, P., 2024. Comprehensive transcriptome, physiological and biochemical analyses reveal that key role of transcription factor WRKY and plant hormone in responding cadmium stress. *J. Environ. Manag.* 367, 121979. <https://doi.org/10.1016/j.jenvman.2024.121979>.
- Xu, H., Liu, P., Wang, C., Wu, S., Dong, C., Lin, Q., Sun, W., Huang, B., Xu, M., Tauqeer, A., Wu, S., 2022. Transcriptional networks regulating suberin and lignin in endodermis link development and ABA response. *Plant Physiol.* 190 (2), 1165–1181. <https://doi.org/10.1093/plphys/kiac298>.
- Yadav, P., Ansari, M.W., Kaula, B.C., Rao, Y.R., Meselmani, M.A., Siddiqui, Z.H., Brajendra, Kumar, S.B., Rani, V., Sarkar, A., Rakwal, R., Gill, S.S., Tuteja, N., 2023. Regulation of ethylene metabolism in tomato under salinity stress involving linkages with important physiological signaling pathways. *Plant Sci.* 334, 111736. <https://doi.org/10.1016/j.plantsci.2023.111736>.
- Yang, J., Song, J., Feng, Y., Cao, Y., Fu, B., Zhang, Z., Ma, N., Li, Q., Hu, T., Wang, Y., Yang, P., 2023. Osmotic stress-induced lignin synthesis is regulated at multiple levels in alfalfa (*Medicago sativa* L.). *Int. J. Biol. Macromol.* 246, 125501. <https://doi.org/10.1016/j.ijbiomac.2023.125501>.
- Yu, Y., Li, J., Song, Y., Zhang, Z., Yu, S., Xu, M., Zhao, Y., 2022. Stimulation versus inhibition: The effect of microplastics on pak choi growth. *Appl. Soil Ecol.* 177, 104505. <https://doi.org/10.1016/j.apsoil.2022.104505>.
- Zhang, K., Wang, M., Li, Y., Zhang, X., Xiao, K., Ma, C., Zhang, X., Zhang, H., Chen, Y., 2024. Wheat (*Triticum aestivum* L.) seedlings performance mainly affected by soil nitrate nitrogen under the stress of polyvinyl chloride microplastics. *Sci. Rep.* 14 (1), 4962. <https://doi.org/10.1038/s41598-024-54838-8>.
- Zahra, N., Hafeez, M.B., Al Shukaily, M., Al-Sadi, A.M., Siddique, K.H., Farooq, M., 2023. Influence of abiotic stresses on disease infestation in plants. *Physiol. Mol. Plant P.* 127, 102125. <https://doi.org/10.1016/j.pmpp.2023.102125>.
- Zhang, W., Hu, Y., Liu, J., Wang, H., Wei, J., Sun, P., Wu, L., Zheng, H., 2020. Progress of ethylene action mechanism and its application on plant type formation in crops. *Saudi J. Biol. Sci.* 27 (6), 1667–1673. <https://doi.org/10.1016/j.sjbs.2019.12.038>.
- Zhang, Y., Qu, X., Li, X., Ren, M., Tong, Y., Wu, X., Sun, Y., Wu, F., Yang, A., Chen, S., 2023. Comprehensive transcriptome and WGCNA analysis reveals the potential function of anthocyanins in low-temperature resistance of a red flower mutant tobacco. *Genomics* 115 (6), 110728. <https://doi.org/10.1016/j.ygeno.2023.110728>.
- Zhao, Q., Dixon, R.A., 2011. Transcriptional networks for lignin biosynthesis: More complex than we thought? *Trends Plant Sci.* 16 (4), 227–233. <https://doi.org/10.1016/j.tplants.2010.12.005>.
- Zhao, X., Gao, S., Ouyang, D., Chen, S., Qiu, C., Qiu, H., Chen, Z., 2023a. Advances on micro/nanoplastics and their effects on the living organisms: a review. *Sci. Total Environ.* 904, 166722. <https://doi.org/10.1016/j.scitotenv.2023.166722>.
- Zhao, X., Wang, Q., Wang, D., Guo, W., Hu, M., Liu, Y., Zhou, G., Chai, G., Zhao, S., Lu, M., 2023b. *PagERF81* regulates lignin biosynthesis and xylem cell differentiation in poplar. *J. Integr. Plant Biol.* 65 (5), 1134–1146. <https://doi.org/10.1111/jipb.13453>.
- Zhou, J., 2021. Microplastics as an emerging threat to plant and soil health in agroecosystems. *Sci. Total Environ.* <https://doi.org/10.1016/j.scitotenv.2021.147444>.